

## **SUPPORTING INFORMATION**

### **A Triangular Three-Dye DNA Switch Capable of Reconfigurable Molecular Logic**

Susan Buckhout-White, Jonathan C. Claussen, Joseph S. Melinger,

Zaire Dunningham, Mario G. Ancona, Ellen R. Goldman, and Igor L. Medintz

**Gel electrophoresis.** DNA was loaded into a 2% agarose gel buffered with 1× TBE buffer (89 mM Tris-borate, 89 mM boric acid, 2 mM EDTA pH 8.3) in TBE running buffer and prestained with gel red intercalating dye (Biotium). The gel was run at 5V/cm for 2 hours on an ice bath. The DNA bands were visualized on a BioRad ChemiDoc XRS+ imaging system.

**Assembly Efficiency.** Gel electropherograms demonstrate that both 2.5×PBS and 1×Tris acetate EDTA (TAE) supplemented with 12.5 mM MgCl<sub>2</sub> display sufficient charge screening for efficient DNA hybridization as evidenced by the bands that appear between 200 to 300 base pairs in both buffer conditions (Figure 2C). The fully formed structure should migrate at a size corresponding to 220-250 base pairs based on just molecular weight alone which is what is indeed observed. However, refining this estimate is complicated by 3-dimensional shape, and full formation was therefore verified by comparison to partially formed structures as shown in the SI. Using image analysis to derive a quantitative comparison of the electropherograms in Figure 2C, the estimated yield for the core structure formed in PBS was around 65%, while the same structure in TAE with Mg<sup>2+</sup> had a yield of close to 80%. As the switch structure is more efficiently formed when 1×TAE with MgCl<sub>2</sub> is used, this buffer was employed in all subsequent work.

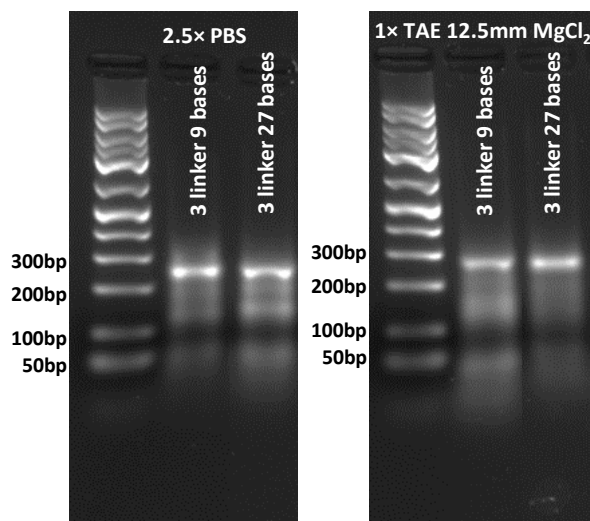


**Figure S1.** Gel electropherograms characterizing the switch assembly formation. Both 2.5×PBS and TAE supplemented with 12.5 mM MgCl<sub>2</sub> were assayed as assembly buffers to assure good formation while minimizing non-specific interactions. Samples were then separated in 2% agarose gels. Both buffers are suitable, but TAE with MgCl<sub>2</sub> was used for its slightly improved performance.

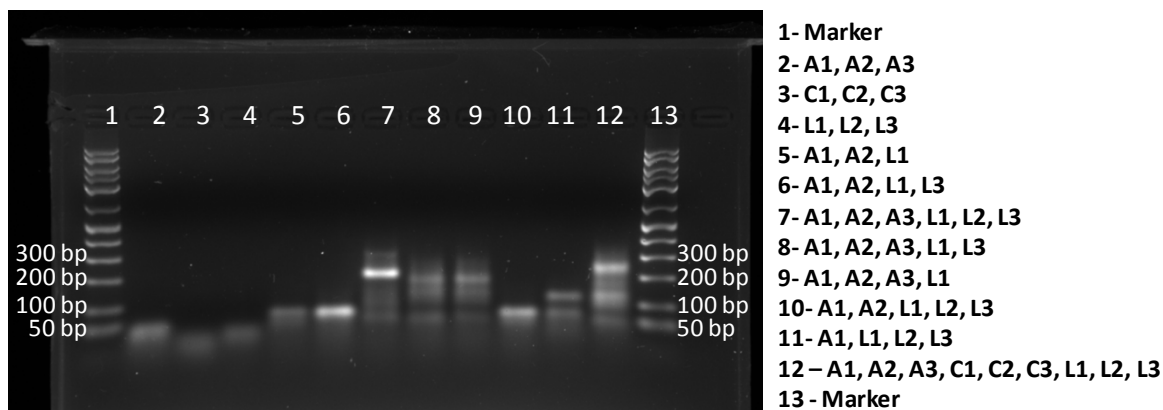
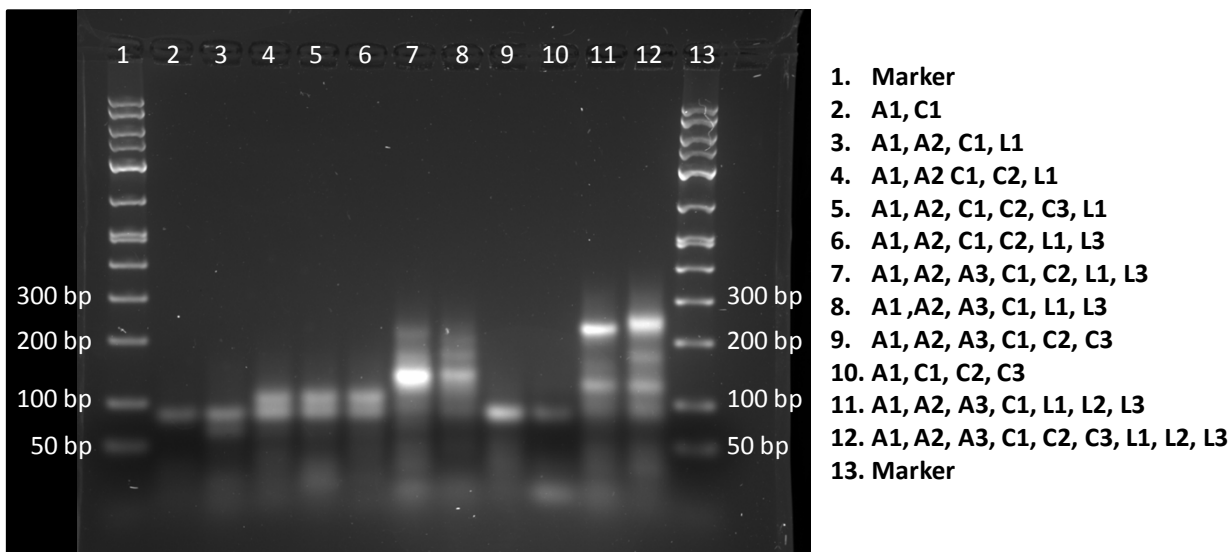
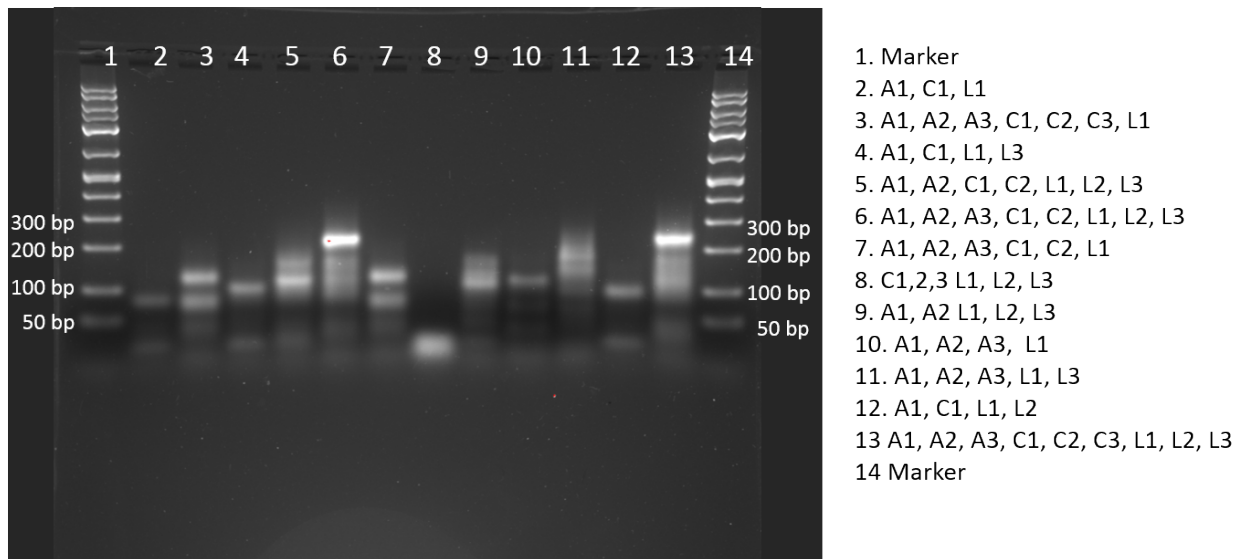


**Figure S2.** Agarose gel of the control structures showing intentional malformation and partial formations used to verify full assembly and assembly efficiency. A = Arm, C = Cap and L = Linker.

**Single Input Logic.** We begin evaluating the potential of the DNA scaffold system by creating single input logic gates, *i.e.*, that process one input to produce a meaningful output. In particular, we devised a simple yes/no buffer gate where the presence or absence of an input produces an ON/1 or OFF/0 response, respectively, see Figure S3, with the input provided by a DNA linker strand (9 base ssDNA linker). Three distinct buffer gates were created by including (or excluding) the 9 base ssDNA linker between the Cy3 and Cy3.5 (L1 switch), the Cy3.5 and Cy5 (L2 switch), or the Cy3 and Cy5 (L3 switch), Figure S3i. These three structures are formed such that each state, whether ON or OFF, is annealed separately. The corresponding PL spectra for the L1, L2, and L3 switches are also displayed in Figure S3i (bottom) with the PL shown for each in the absence (yellow spectra) and presence of the linker (blue spectra). These PL spectra are converted into a Boolean logic output by quantizing the ratio of the PL peak height of the FRET acceptor dye to that of the donor (Figure S3iii). In the case of the L2 and L3 switches, a PL ratio threshold of 0.2 was established so that PL peak height ratios above 0.2 are converted to ON/1 outputs while those below become OFF/0. For the L1 switch the PL ratio threshold was set to 0.5 in order to compensate for direct excitation of the Cy3.5 dye. This latter adjustment highlights an important underlying point about such multi-dye constructs and FRET, namely that some donor-acceptor combinations will be more susceptible to direct acceptor excitation or more efficient than others at the same nominal distance, and the assignment of thresholds needs to consider this and not remain static assuming one value will suffice for all.

**Figure S3. Two-arm single input device.** **i)** Schematic showing the formation of the three different one linker (input) structures along with respective spectra for each when the linker is present (blue) or not (yellow). **ii)** These spectra correspond to a buffer gate that reflects the yes/no (ON/1 or OFF/0) status of the 9 base linker. **iii)** Shows the output signal and assigned output state for each structure. Note, that due to the close spectral overlap of Cy3 and Cy3.5, the designated threshold must be set higher than the other two dye sets. Error bars represent the standard deviation of at least  $n = 3$  experiments.

**Table SI. Fluorophore photophysical and FRET properties.**

Fluorophores	Quantum yield	Extinction coefficient (M <sup>-1</sup> cm <sup>-1</sup> )	$\lambda_{\max}$	$\lambda_{\max}$	<sup>1</sup> R <sub>0</sub> in Å / J(λ) in cm <sup>3</sup> M <sup>-1</sup>		
			absorption	emission	Cy3	Cy3.5	Cy5
<b>Cy3</b>	0.15	150,000	550 nm	570 nm	47 / 3.68e <sup>-13</sup>	53 / 8.01e <sup>-13</sup>	54 / 9.37e <sup>-13</sup>
<b>Cy3.5</b>	0.15	150,000	581 nm	596 nm	---	44 / 2.70e <sup>-13</sup>	60 / 1.69e <sup>-12</sup>
<b>Cy5</b>	0.28	250,000	649 nm	670 nm	---	---	65 / 1.39e <sup>-12</sup>

<sup>1</sup>R<sub>0</sub> and J(λ) values are averages calculated from the spectra of all dye-labeled DNA used in this study.

**Table SII. DNA sequences**

Name	Sequence	Modification	T <sub>m</sub> (1X TAE 12.5 mM MgCl <sub>2</sub> )	Source
<b>Arm 1</b>	GGTTCAGCCGCAATCCGGCACAGCTATAATAA*GA GTTTGATGAAATGGAGCGGACGTGAGATGG	*Internal Cy3	79.0	IDT
<b>Arm2</b>	GCAAGACTCGTGCTCAGGTCCTAAGTTGGTTCT*AC CGCATGGTATATGGGGCTTACGGTGGTGCG	*Internal Cy3.5	79.7	Operon
<b>Arm 3</b>	GGATCAGAGCTGGACGGGAGCCTATCGGGTAG*TT ATGTTGTTTCGCTGGTGTACTGCATCCAGG	*Internal Cy5	79.3	IDT
<b>Cap 1</b>	CCATCTCACGTCCGCTGGATTGCGGCTGAACC		76.7	IDT
<b>Cap 2</b>	CGCACCACCGTAAGCCTGAGCACGAGTCTTGC		76.5	IDT

<b>Cap 3</b>	CCTGGATGCAGTAACACGTCCAGCTCTGATCC	73.9	IDT
<b>Link1 9 base spacing</b>	GCCGGAGACCATATACCATGCGGTAAAAAAAATT ATTATAGCTGTGCC	75.2	IDT
<b>Link1 18 base spacing</b>	GCCGGAGACCATATACCATGCGGTAAAAAAA AAAAAAAATTATTATAGCTGTGCC	76.0	IDT
<b>Link1 27 base spacing</b>	GCCGGAGACCATATACCATGCGGTAAAAAAA AAAAAAAAAAAAAAAAAATTATTATAGCTGTGCC	76.9	IDT
<b>Link2 9 base spacing</b>	CCTGTACGCCAGCGAACAAACATAATAATAAGA ACCAACTTAGGACC	74.5	IDT
<b>Link2 18 base spacing</b>	CCTGTACGCCAGCGAACAAACATAATAATAATA ATAATAAGAACCAACTTAGGACC	74.4	IDT
<b>Link2 27 base spacing</b>	CCTGTACGCCAGCGAACAAACATAATAATAATA ATAATAATAATAAGAACCAACTTAGGACC	74.7	IDT
<b>Link3 9 base spacing</b>	GATACGGACCATTTCATCAAACCTCAAATAAATTCT ACCCGATAGGCTCC	74.4	IDT
<b>Link3 18 base spacing</b>	GATACGGACCATTTCATCAAACCTCAAATAAATTAA ATAAATTCTACCCGATAGGCTCC	74.7	IDT
<b>Link3 27 base spacing</b>	GATACGGACCATTTCATCAAACCTCAAATAAATTAA ATAAATTAAATAAATTCTACCCGATAGGCTCC	75.2	IDT
<b>Link1 9 base comp</b>	GGCACAGCTATAATAATTTTTTTTTTACCGCATGGTA TATGGTCTCCGGC	75.2	IDT
<b>Link1 18 base comp</b>	GGCACAGCTATAATAATTTTTTTTTTTTTTTTACC GCATGGTATATGGTCTCCGGC	76.0	IDT
<b>Link1 27 base comp</b>	GGCACAGCTATAATAATTTTTTTTTTTTTTTTTTT TTTTTACCGCATGGTATATGGTCTCCGGC	76.9	IDT
<b>Link2 9 base comp</b>	GGTCCTAAGTTGGTTCTTATTATTATTATGTTGTT GCTGGCGTACAGG	74.5	IDT
<b>Link2 18 base comp</b>	GGTCCTAAGTTGGTTCTTATTATTATTATTATT ATGTTGTTTCGCTGGCGTACAGG	74.4	IDT

<b>Link2</b> <b>27 base comp</b>	GGTCCTAAGTTGGTTCTTATTATTATTATTATTATT ATTATTATTATGTTGTTTCGCTGGCGTACAGG	74.7	IDT
<b>Link3</b> <b>9 base comp</b>	GGAGCCTATCGGGTAGAATTTATTTGAGTTTGATG AAATGGTCCGTATC	74.4	IDT
<b>Link3</b> <b>18 base comp</b>	GGAGCCTATCGGGTAGAATTTATTTAATTTATTTGA GTTTGATGAAATGGTCCGTATC	74.7	IDT
<b>Link3</b> <b>27 base comp</b>	GGAGCCTATCGGGTAGAATTTATTTAATTTATTTAA TTTATTTGAGTTTGATGAAATGGTCCGTATC	75.2	IDT

\*in sequence indicates modifier placement

**Table SIII. Data averages and standard deviations for the three linker logic.**

Permutation			Average			Std. Dev.		
L1	L2	L3	606/564	664/606	664/564	606/564	664/606	664/564
0	0	0	0.337	0.098	0.033	0.045	0.021	0.007
0	0	27	0.466	0.780	0.367	0.073	0.077	0.084
0	9	0	0.199	0.775	0.153	0.024	0.084	0.007
0	9	27	0.271	1.859	0.503	0.013	0.075	0.012
9	0	0	0.864	0.069	0.059	0.104	0.013	0.011
9	0	27	1.002	0.527	0.530	0.050	0.066	0.080
9	9	0	0.591	1.114	0.663	0.050	0.165	0.145
9	9	27	0.449	1.867	0.850	0.070	0.180	0.209